NASA Technical Memorandum 82793

Metal Honeycomb to Porous Wireform Substrate Diffusion Bond Evaluation

A. Vary, P. E. Moorhead,
and D. R. Hull
Lewis Research Center
Cleveland, Ohio

(NASA-TM-82793) METAL HONEYCOMB TO POROUS WIREFORM SUBSTRATE DIFFUSION BOND EVALUATION (NASA) 12 p HC A02/MF A01 CSCL 14D

N82-18612

Unclas
G3/38 09125

Prepared for the
Spring Conference of the American Society
for Nondestructive Testing
Boston, Massachusetts, March 22-25, 1982

NASA

METAL HONEYCOMB TO POROUS WIREFORM SUBSTRATE

DIFFUSION BOND EVALUATION

by A. Vary, P. E. Moorhead, and D. R. Hull

National Aeronautics and Space Administration
Lewis Research Center
Cleveland, Ohio 44135

ABSTRACT

Two somewhat novel nondestructive techniques were used to evaluate diffusion bond quality between a metal foil honeycomb and porous wireform substrate. The two techniques, cryographics and acousto-ultrasonics, were found to be complementary in revealing variations of bond integrity and quality in shroud segments from an experimental aircraft turbine engine. Because of gross porosity and adverse geometric factors, conventional ultrasonic and other techniques were determined to be inappropriate. The techniques described herein appear to merit consideration for use in similar circumstances.

INTRODUCTION

Evaluation of diffusion or adhesive bond quality can be a challenging nondestructive testing problem when it involves either similar or dissimilar but otherwise continuous solids. The difficulty is aggravated when both materials being interfaced are porous or discontinuous like honeycomb and wire mesh. Lack of continuous media for signal transmission to and from the bondline imposes severe constraints on technique selection.

E-959

Pulse-echo ultrasonics is usually the method of choice in attempts to evaluate the integrity and quality of both adhesive and diffusion bonds. The case treated herein involves bond integrity between a metal honeycomb outer layer and a porous wireform, "poralloy", substrate. The usual ultrasonic methods were found inadequate due to the gross porosity and geometric factors that made it impossible to recover appropriate signals. Instead, bond evaluation was accomplished by two somewhat novel techniques: cryographics and acousto-ultrasonics. The purpose of this report is to describe the application of cryographics and acousto-ultrasonics to evaluate bonding integrity in porous media such as the honeycomb/poralloy combinations used for shrouds in a NASA Lewis turbine test facility.

TEST ARTICLE

One of the shroud segments evaluated for diffusion bond integrity is shown in Fig. 1. Eight shroud segments identical to the one shown comprise a complete circular assembly in an experimental, high pressure aircraft turbine test facility at NASA's Lewis Research Center. The shroud surrounds a high pressure turbine stage in which only small clearances are allowed between the blade tips and shroud.

During operation, cooling gas enters through holes in the back of the shroud body and exits through the honeycomb. After distribution by channels machined in the shroud body, the cooling gas is conducted through a porous wireform multi-layer, illustrated in Fig. 2. The honeycomb through which the gas exists consists of corrugated metal foil spot welded together to form the individual cells. As indicated in Fig. 2 the honeycomb layer is diffusion bonded to the wireform substrate.

The primary purpose of the honeycomb is to provide an abradable surface in case eccentricities cause the blade tips to rub against the shroud. Figure 3 illustrates the severe damage incurred by honeycomb that had separated from the wireform substrate due to poor bonding. In addition to the unacceptable entrainment of large pieces of debris into the gas stream, this damage seriously compromised effective sealing against axial leakage.

TECHNIQUE SELECTION

Although contact pulse echo ultrasonics can indicate bondline integrity (Refs. 1 and 2) it was rendered impractical by the geometry of the shroud segment and its internal structure and porosity. Attempts to recover bondline signals by coupling to the back surface would be frustrated by the discontinuities due to the gas distribution channels (Fig. 4) in addition to the wireform porosity. Use of immersion scanning, although overcoming problems of direct contact, was ruled out because of anomalous effects that would arise from water infiltration in the porous structure.

Use of a silicon rubber buffered transducer (as in Fig. 4) permits direct, dry contact. With a 1-centimeter diameter by 0.15-centimeter thick buffer, good coupling is reproducibly established with approximately 4.5-kilograms force. The buffer comforms to the shroud curvature and honeycomb cells. However, attempts to use a single transducer in pulse-echo mode proved futile for distinguishing between good bonds and known disbonds. It was found that the use of two transducers in the send-receive configuration shown in Figs. 4 and 5 gave excellent results using the acousto-ultrasonic technique described hereinafter. This technique yielded a quantitative ranking of bond integrity.

Corroborative techniques such as thermography and holography were considered (Refs. 3 and 4) but judged inappropriate because of the elaborate procedures that would be involved. Nevertheless, some form of imaging technique was deemed necessary to supplement the limited number of readings practicable with acousto-ultrasonics in the contact mode that was used. An easily accomplished and rapid imaging technique called cryographics was contrived, as explained in the next section.

CRYOGRAPHICS

The cryographic technique is a variation on thermography. In the present case a thermal pattern is generated as the test article is warmed to room temperature after being isothermally cooled by immersion in liquid nitrogen. Under ambient conditions of humidity, thermal patterns are revealed by frost formation as opposed, for example, to color changes that would be obtained by thermography with liquid crystals (Ref. 5).

For the shroud segments a frost pattern appeared on the honeycomb over regions of disbond, as illustrated in Fig. 3. Under the ambient conditions in our laboratory, 21° C (70° F) and 40 percent humidity (approximately) during testing, a well-defined frost pattern emerged within about 4 minutes. A liquid nitrogen immersion time of roughly 5 minutes was found adequate for the shroud segments. After removal from the liquid nitrogen bath, excess fluid rapidly drained out of the test piece and any residue remaining had no apparent effect.

It should be noted that the relatively uniform reflectance of the honeycomb over regions not obviously damaged aids in discerning subleties in the emerging frost pattern. Also, it was determined in advance that for the high-nickel-base alloys that comprised the shroud segment no adverse effects would be engendered by the liquid nitrogen immersion.

ACOUSTO-ULTRASONICS

Detailed aspects of the acousto-ultrasonic technique have been described elsewhere (Refs. 6 and 7). The essence of acousto-ultrasonics is in the combination of complementary features of acoustic emission and ultrasonics. Acousto-ultrasonics affords a method for sensing and measuring ultrasonic pulses after pronounced attenuation and scattering by material geometry and porosity factors as in the present case. In the configuration illustrated in Figs. 4 and 5, an acoustic emission sensor and circuitry receive the signals that arise after input by the sending transducer. The acoustic emission circuitry provides the necessary amplification, sensitivity, and processing methods for analyzing the resultant signals.

The physical arrangement of the transducers is such that the signals sensed by the receiving transducer have propagated across the width of the honeycomb. The character of the resultant waveform is influenced in part by the boundary conditions between the honeycomb and wireform substrate. Although the waveform is quite complex, it can be quantitized in terms of a "stress wave factor". The stress wave factor is essentially a relative measure of stress wave propagation energy. This quantity will be larger for good bonds and smaller for poor bonds.

Examples of the variation of the stress wave factor measured in terms of an energy curve are given in Fig. 6. The energy curve is proportional to a volts (squared) seconds analog of the acousto-ultrasonic waveform. Because of the particular transducer spacing and orientation used (Fig. 4), the energy variations indicate the cumulative effect of the several types of bond conditions that may exist in the volume included between the transducers.

PROCEDURE AND RESULTS

Fifteen equally-spaced acousto-ultrasonic measurements were made on each shroud segment. This gave a profile of bonding variations in the circumferential direction. Each segment was subsequently immersed in liquid nitrogen and the frost pattern that developed was photographed. Representative results are shown in Fig. 7.

The graph in Fig. 7 is a plot of the acousto-ultrasonic stress wave factor against each of fifteen positions marked off along the edge of the segment. In this instance the instrument settings were adjusted to rate each position on a scale of 300. It is evident from Fig. 7 that the lowest values of the stress wave factor corresponded to the two areas with the poorest bonding according to the frost pattern.

Altogether, sixteen shroud segments were inspected. Of these, eight were previously used in the high pressure turbine facility and had been removed after some were damaged, as in Fig. 3. A second set of eight segments had not been previously used. When evaluated, these were found to have significant variations in bond quality. In one of the unused segments there was a total lack of bonding over an approximately 5-centimeter-long region near the edge of the honeycomb. This was initially revealed by a simple coin-tap test and then confirmed by probing with a knife blade. This information helped in setting a baseline for the lowest stress wave factor reading.

Typically, all segments, both new and used, exhibited the strongest bonding and greatest stress wave factor at either end, i.e., in the region of positions 1 - 3 and 13 - 15. From each end inward the bond quality worsened, usually reaching a minimum near the center. The acousto-ultrasonic and cryographic indications were confirmed by peel tests on previously-used segments that had not sustained any obvious damage. Starting at either end (positions 1 or 15) considerable force was required to pry the honeycomb loose from the wireform substrate. Approaching the center of the segment (positions 5 - 10) the honeycomb peeled off easily in direct agreement with the nondestructive indications. After peeling, the substrate had a roughness pattern that corresponded exactly with the cryographic indications, the smoothest areas being those with either poor or no bonding.

Obviously, poor or no bonding between the honeycomb and wireform resulted in lower energy transmission and hence lower values of the stress wave factor. Any improvement in bonding should show an increase in the stress wave factor, as in Fig. 8. That figure illustrates the improvement in bonding obtained by making 600 closely-space spot welds over the honeycomb area. These spot welds were made through the honeycomb to increase the bonded area of the honeycomb-wireform interface.

DISCUSSION

Results of the nondestructive evaluations and subsequent destructive tests made it apparent that there were deficiencies in the fabrication process used to make the shroud segments. The overall bond quality between the honeycomb and wireform substrate was poor. This was partly ascribable to curvature of the segments and consequent difficulty in maintaining uniform pressure and intimate contact at the bond interface. The diffusion bonding process included a consumable metal foil filler. This still failed to assure uniform bonding.

Both nondestructive evaluation methodologies described herein had shortcomings. The acousto-ultrasonic method that was used gave only a relatively crude indication of bond integrity. The estimated error in the stress wave factor reading was roughly ±10 percent. A poor bond or discontinuity just under the transducers tended to give a lower reading than a similar bond flaw between the transducers. The limited number of readings per segment, i.e., 15 equally-spaced readings over the 19-centimeter (7.5-inch) length, gave an adequate but coarse spatial resolution. This particular shortcoming was covered by the cryographic method which revealed bonding patterns with high spatial resolution.

The cryographic frost patterns gave good indications of variations in bonding. However, it was noticed that a shroud segment with uniformly poor bonding would not give a good differential frost pattern and could be misinterpreted as being of good general quality. This misinterpretation is avoidable by comparing the cryographic results with the acousto-ultrasonic readings.

The basis of cryographic frost pattern formation is straightforward. Once an object is isothermally cooled, it is obvious that non-uniformities will be revealed during warm-up to room temperature. The frost pattern that develops depends on the thermal conductivity and heat capacity of the materials involved. In the present case, unbonded or poorly-bonded areas reached a "frosting" temperature sooner than well-bonded areas. This is consistent with the expectation that poorly-attached material warms sooner than material in good thermal contact with the cold heat sink provided by the shroud body.

The basis of acousto-ultrasonic indications is complex. Obviously, the wave propagation path from the sending to receiving transducer is tortuous. Any signal sensed by the receiver will have experienced multiple reflections at the various boundaries encountered. The honeycomb foil and wireform substrate components act as waveguides in conducting the ultrasonic energy. Judging from the typical frequency spectra, as in Fig. 6, most of this energy propagated with wavelengths greater than the dimensions of the foil or wires that comprised the materials. This indicates that some form of scattering was involved in wave propagation. One of the difficulties in analyzing the wave propagation is that of determining how the energy is partitioned between the honeycomb and wireform.

The results shown in Fig. 8 can be interpreted as indicating that increases in the stress wave factor correspond to increases in the number of well-bonded points of contact at the honeycomb-wireform interface. From this it can be inferred that the wireform substrate is more efficient in transmitting acousto-ultrasonic waves than the honeycomb (for the transducer configuration in Fig. 4). This latter inference was readily confirmed by a separate test involving transducers coupled to a sample of the wireform multi-layer alone.

CONCLUSION

Nondestructive evaluation of bond quality between a metal foil honeycomb and wireform substrate was successfully accomplished by two complementary techniques: acousto-ultrasonics and cryographics. The acousto-ultrasonic readings proved quite satisfactory for numerically rating bonding quality while cryographic frost patterns rendered detailed imagings of bonding variations. The results obtained with the two techniques indicate that they merit consideration in similar situations where either porosity or geometric factors preclude the use of other more conventional nondestructive methods.

REFERENCES

1. E. Segal and J. L. Rose, "Nondestructive Testing Techniques for Adhesive Bond Joints," Research Techniques in Nondestructive Testing, Vol. 4, 1980, p. 275. R. S. Sharpe, ed., Academic Press, London.
2. J. C. Couchman, B. G. W. Yee, and F. H. Chang, "Adhesive Bond Strength Classifier," Materials Evaluation, Vol. 37, No. 5, Sept. 1979, p. 48-50.

3. A. E. Ennos, "Optical Holography and Coherent Light Techniques," Research Techniques in Nondestructive Testing, 1970, p. 155. R. S. Sharpe, ed., Academic Press, London.
4. R. E. Englehardt and W. A. Hewgley, "Thermal and Infrared Testing," Nondestructive Testing - A Survey, NASA SP-5113, 1973, p. 119-140.
5. J. H. Williams, Jr., S. H. Mansouri, and S. S. Lee, "Thermal Nondestructive Testing of Fiberglass Laminates Using Liquid Crystals," British Journal of Nondestructive Testing, Vol. 22, No. 4, July 1980, p. 184-190.
6. A. Vary, "Concepts and Techniques for Ultrasonic Evaluation of Material Mechanical Properties," Mechanics of Nondestructive Testing, 1980, p. 123. W. W. Stinchcomb, ed., Plenum Publishing, New York.
7. A. Vary, "Acousto-Ultrasonic Characterization of Fiber Reinforced Composites," NASA TM-82651, 1981.

ORIGINAL PAGE
BLACK AND WHITE PHOTOGRAPH

(a) FRONT VIEW.

(b) END VIEW.

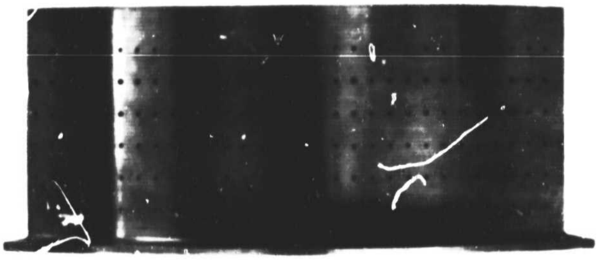

(c) BACK VIEW.

Figure 1. - Views of shroud segment. Layer of honeycomb formed from metal foil is diffusion bonded to wireform porous metal layer, details in figures 2 and 4.

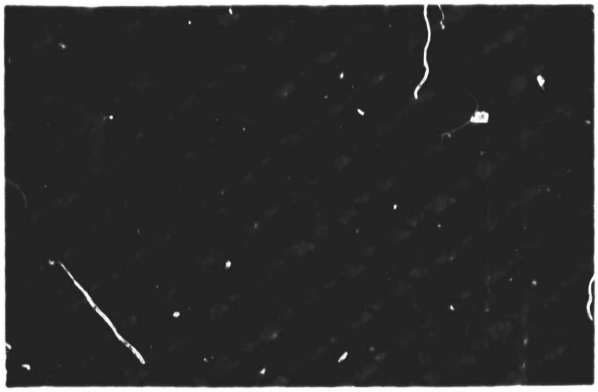

(a) WIREFORM POROUS METAL MULTI-LAYER.

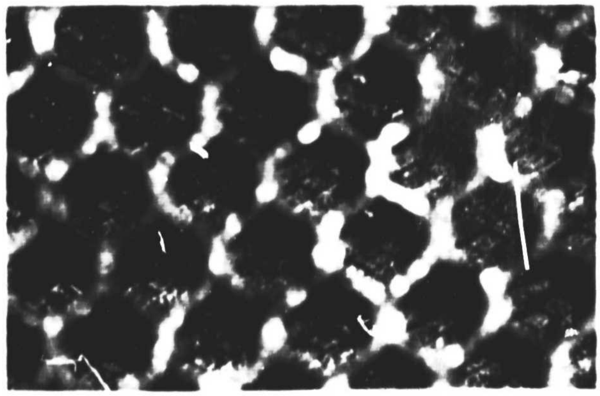

(b) HONEYCOMB BONDED TO WIREFORM.

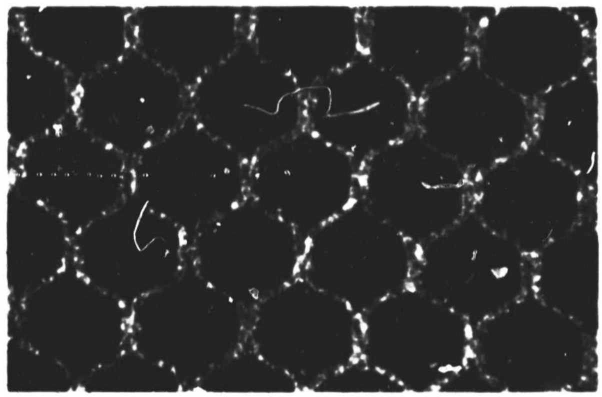

(c) METAL FOIL HONEYCOMB LAYER.

Figure 2. - Details of wireform substrate and diffusion bonded honeycomb. Honeycomb cell size is 0.1-centimeter and foil (web) thickness is 0.01-centimeter, approximately.

ORIGINAL PAGE
BLACK AND WHITE PHOTOGRAPH

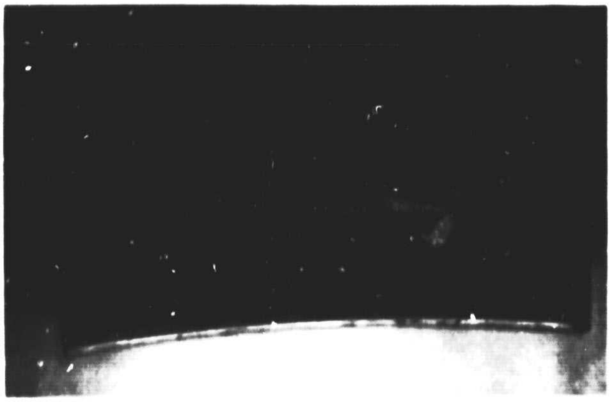

(a) FROST PATTERN ON LOOSE HONEYCOMB 1.5 min AFTER REMOVAL FROM LN_2.

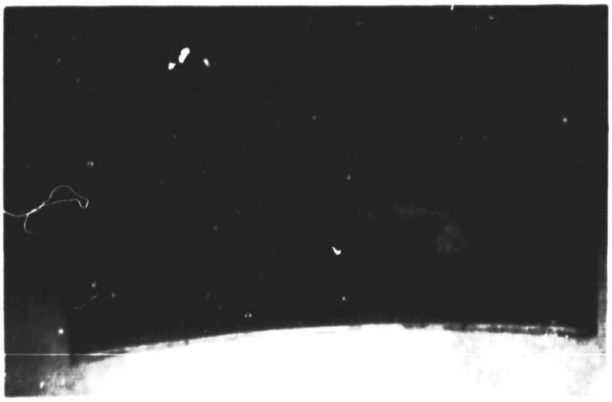

(b) FROST PATTERN ON LOOSE HONEYCOMB 2.5 min AFTER REMOVAL FROM LN_2.

Figure 3. - Example of damaged honeycomb separated from wireform substrate due to poor bonding. Whitened areas are frost pattern after dipping in liquid nitrogen.

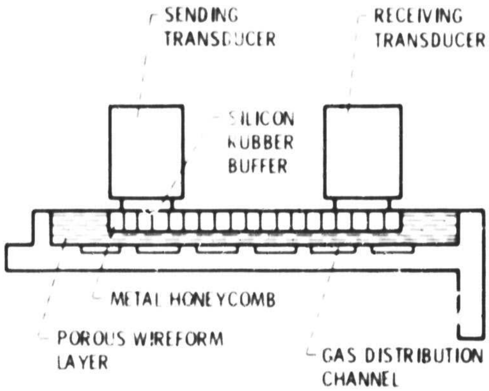

Figure 4. - Details of transducer arrangement and cross section of shroud segment.

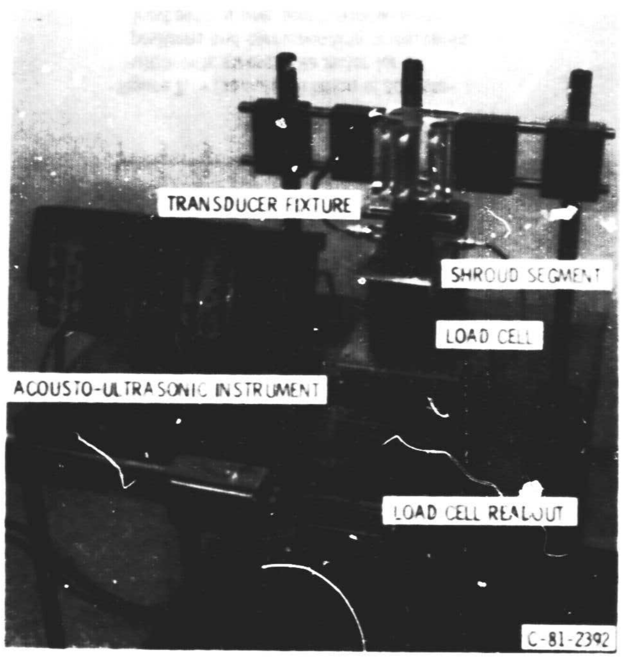

Figure 5. - Apparatus for acousto-ultrasonic evaluation of honeycomb-to-wireform bond quality. (To assure reproducible coupling the applied force was monitored by means of the load cell and readout.)

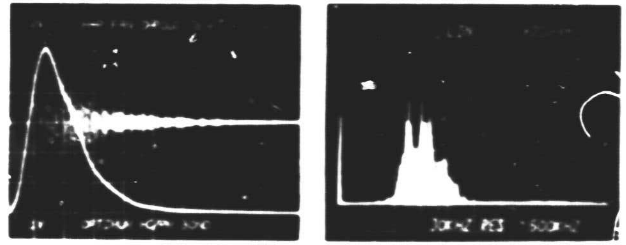

(a) OPTIMUM BOND OVER ENTIRE INTERFACE BETWEEN TRANSDUCERS.

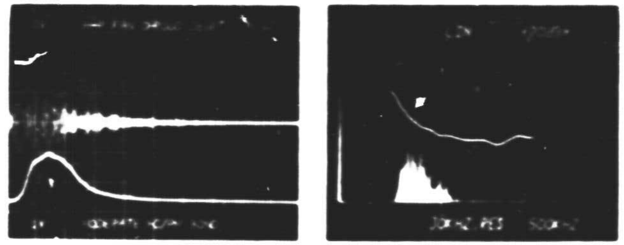

(b) INFERIOR BOND IN ZONE MIDWAY BETWEEN TRANSDUCERS.

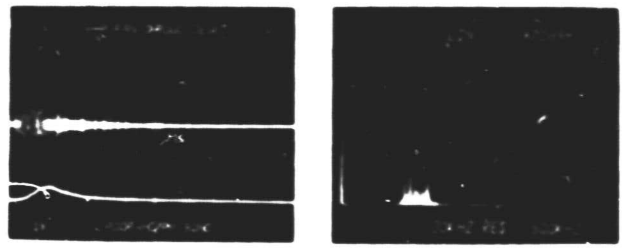

(c) INFERIOR BOND IN ZONE JUST BENEATH ONE TRANSDUCER.

Figure 6. - Effect of honeycomb-to-wireform bond quality on acousto-ultrasonic signal. Energy curve superimposed on CRT trace of signal (left) and ultrasonic frequency spectrum of signal (right).

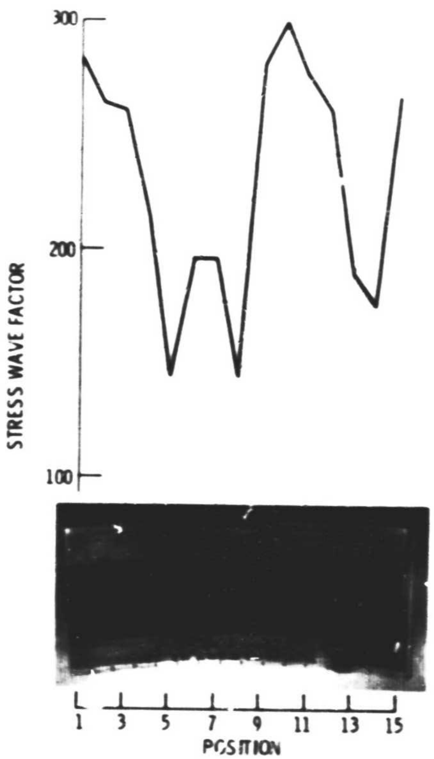

Figure 7. - Example variation of acousto-ultrasonic stress wave factor for 15 positions and corresponding cryographic frost pattern over poorly bonded areas (lighter grey).

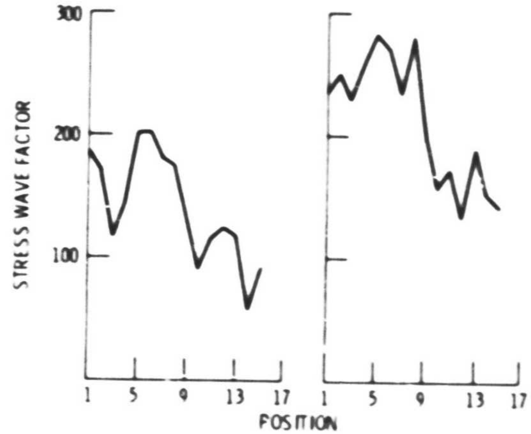

(a) As-received shroud segment.

(b) Segment after spot-welding.

Figure 8. - Comparison of stress wave factor profiles for a shroud segment before and after spot-welding to improve bond between honeycomb and wireform. Approximately 600 regularly-spaced spot welds were made through the honeycomb to increase metallurgical bonding at the honeycomb-wireform interface.